Journal of Alloys and Compounds 517 (2012) 14–19

Contents lists available at SciVerse ScienceDirect

Journal of Alloys and Compounds

journal homepage: www.elsevier.com/locate/jallcom

Synthesis of $CuInSe_2$ films via selenizing the Cu–In alloy-containing nanopowders

Shih-Hsien Liu, Fu-Shan Chen, Chung-Hsin Lu*

Department of Chemical Engineering, National Taiwan University, Taipei, Taiwan, ROC

ARTICLE INFO

Article history:
Received 11 July 2011
Received in revised form
22 November 2011
Accepted 23 November 2011
Available online 30 November 2011

Keywords:
Nanopowders
$NaBH_4$
$CuInSe_2$
Solar cells

ABSTRACT

$CuInSe_2$ thin films were prepared employing nanopowders consisting of Cu–In alloys and In as the precursors of selenization. The nanopowders were synthesized via the chemical reduction method using $NaBH_4$ as the reductant and water as the solvent. On selenization at 350 °C, $CuInSe_2$ started to form along with the intermediate compounds of copper selenides. The sizes of the grains in the thin films were significantly increased at 450 °C because of the existence of Cu–Se phases. When the selenization temperature was raised to 550 °C, the densified $CuInSe_2$ films with a grain size of around 2 μm were observed. The formation and uniformity of single-phase $CuInSe_2$ throughout the thin film were verified via grazing incident X-ray diffraction. The Raman spectroscopy and the Rietveld refinement method confirmed the pure chalcopyrite phase of $CuInSe_2$. The band gap of the $CuInSe_2$ thin film was measured to be 0.97 eV via the UV–visible–NIR spectroscopy. The $CuInSe_2$ thin-film solar cells exhibited a photovoltaic conversion efficiency of 1.47% under AM 1.5 G illumination.

1. Introduction

Thin-film solar cells have been extensively developed as the second-generation solar cells due to the reduced cost and increasing energy demand. Among various types of thin-film solar cells, copper indium diselenide with chalcopyrite structure (α-$CuInSe_2$) is regarded as a promising material in the absorber layers of the thin-film solar cells because of its high absorption coefficient ($\sim 10^5\ cm^{-1}$) and direct band gap [1]. Ga (gallium) is usually doped into $CuInSe_2$ to tune the band gap of $CuInSe_2$ from 1.0 to 1.7 eV for achieving improved efficiencies in Cu(In, Ga)Se_2 solar cells [2]. The overall photovoltaic conversion efficiency of Cu(In, Ga)Se_2-based solar cells has been reported to be comparable to that of multicrystalline-Si colar cells [3].

Cu(In, Ga)Se_2 thin films are usually prepared via the vacuum processes such as the co-evaporation process and the sputtering method [4,5]. However, expensive and complicated equipments are required in the vacuum processes. Low utilization rate of source materials (Cu, In, Ga, Se) is also a disadvantage. To reduce the cost and conserve the usage of starting materials, developing a non-vacuum process is necessary. Different kinds of non-vacuum methods have been utilized to prepare Cu(In, Ga)Se_2 materials. These methods include the synthesis of Cu–In alloys via the melt atomization technique [6,7], the preparation of inks containing copper and indium oxide or nitride [8,9], mechanochemical processing (MCP) [10] and the electrodeposition [11]. In addition, the preparation of a solution with copper and indium compounds and hydrazine was also proposed [12,13]. However, shortcomings have been found in the above methods such as the requirement of high temperatures and specific atmosphere, reduction of the thin films at high temperatures before selenization, and the utilization of highly toxic and dangerously unstable hydrazine.

To overcome the drawbacks of the above mentioned non-vacuum methods, the chemical reduction method using sodium borohydride ($NaBH_4$) as the reducing agent was employed. The chemical reduction method is a low-cost process, and it is considered to be suitable for industrial manufacture [14]. The $NaBH_4$-assisted chemical reduction method has been utilized to synthesize nanosized metals effectively [15,16]. Cu–In alloys have been synthesized via $NaBH_4$-assisted chemical reduction method [17,18]. It is worth mentioning that the study concerning the selenization reaction of $CuInSe_2$ films employing Cu–In alloys has not yet been investigated in detail. In this study, nanopowders with Cu–In alloys and In were rapidly synthesized in water at relatively low temperatures in ambient conditions using low-toxic $NaBH_4$. Additionally, triethylamine (TEA) was used as a particle stabilizer for inhibiting the oxidation of the nanopowders. The thin films coated with the obtained nanopowders were selenized to form dense $CuInSe_2$ thin films. The compact $CuInSe_2$ thin films were synthesize to fabricate $CuInSe_2$ solar cells. The phases and sizes of the prepared powders were examined. The influence of the selenization conditions on the formed phases and microstructures of the selenized thin films were investigated. The photovoltaic characteristics of the $CuInSe_2$ thin-film solar cell were measured.

* Corresponding author. Tel.: +886 2 23651428; fax: +886 2 23623040.
E-mail address: chlu@ntu.edu.tw (C.-H. Lu).

0925-8388/$ – see front matter © 2011 Elsevier B.V. All rights reserved.
doi:10.1016/j.jallcom.2011.11.105

2. Experimental

Cu–In alloy-containing nanopowders were synthesized via the $NaBH_4$-assisted chemical reduction method. Copper (II) chloride dihydrate ($CuCl_2{\cdot}2H_2O$) and indium chloride tetrahydrate ($InCl_3{\cdot}4H_2O$) were dissolved in deionized (DI) water. The molar ratio of $CuCl_2{\cdot}2H_2O$ to $InCl_3{\cdot}4H_2O$ was fixed at 1:1. After stirring, sodium borohydride ($NaBH_4$) was gradually added into the above solution, followed by the addition of triethylamine (TEA). The molar ratios of metal ions (Cu^{2+} and In^{3+}) to $NaBH_4$ to TEA were fixed at 1:10:10. After stirring, the obtained powders were washed with methanol, concentrated through centrifugation, and dried at 70 °C.

The synthesized powders were mixed thoroughly with polyoxyethylene-(10)-octylphenyl ether (OP-10) (surfactant) and 1-hexanol (solvent) to prepare the ink. The weight ratios of the powders to OP-10 to 1-hexanol were set at 6: 1: 13. Subsequently, two stripes of a 3 M scotch tape were applied to both sides of the soda lime glass (SLG) substrates for adjusting the thickness of the precursor films. Subsequently, the prepared ink in this study was then coated on the above substrate via the doctor-blading route using a glass rod. The desiccated thin films were selenized at temperatures ranging from 250 °C to 550 °C for 30 min in a tube furnace to prepare $CuInSe_2$ thin films. Se powder was used as the Se source and 5% H_2/95% N_2 was employed as the gas flow.

For the fabrication of $CuInSe_2$ thin-film solar cells, the ink was also coated on Mo-coated SLG substrates via a doctor-blading method, followed by selenization of desiccated thin films in 5% H_2/95% N_2. CdS was then coated on $CuInSe_2$ thin films via the chemical bath deposition (CBD). After covering $CuInSe_2$ with CdS, i-ZnO was sputtered onto CdS, and ITO was then sputtered onto i-ZnO.

The phases of the obtained powders and thin films were analyzed using an X-ray diffractometer (XRD, Philips X'Pert/MPD) with Cu K_α radiation at 45 kV and 40 mA. The crystalline structure of thin films in different depths was characterized via the grazing incident X-ray diffraction (GIXD). The particle sizes of the prepared powders were examined utilizing a transmission electron microscope (TEM, Hitachi H-7100). The morphology and grain sizes of the obtained thin films were investigated employing a scanning electron microscope (SEM, Hitachi S-800). The compositions of the obtained films were analyzed using energy dispersive X-ray spectrometer (EDS, NovaTM NanoSEM 230). The crystalline structure of the thin films was characterized using a Raman spectroscope (HORIBA Jobin Yvon T64000) performed in a backscattering configuration with Ar ion laser (wavelength 514.5 nm) as a light excitation source. The absorbance of the thin films in the UV–visible–NIR region was analyzed utilizing an UV–visible–NIR spectrophotometer (JASCO V-570). The current–voltage characteristics of solar cells were measured employing an AM 1.5 G (100 mW/cm^2) solar simulator (Hong-Ming Tech.).

3. Result and discussion

3.1. Characterization and microstructures of the prepared nanopowders

The nanopowders were synthesized rapidly via the $NaBH_4$-assisted chemical reduction method at relatively low temperature in ambient atmosphere. The X-ray diffraction patterns of the prepared nanopowders are illustrated in Fig. 1. It is found that CuIn and Cu_2In were formed after the co-reduction of Cu^{2+} and In^{3+} in water using $NaBH_4$ as the reducing agent. In addition to Cu–In alloy phases, indium (In) was also observed. The XRD patterns of CuIn, Cu_2In, and In were consistent with the reported data (ICDD Card Nos. 35-1150, 42-1475, and 85-1409, respectively). The reaction during the reduction process is related to the standard reduction potentials (E^0) of Cu^{2+}/Cu, In^{3+}/In, and $B(OH)_3/BH_4^-$ [19]. The values of E^0 for Cu^{2+}/Cu and In^{3+}/In are 0.34 V and −0.34 V, respectively, which are higher than that of $B(OH)_3/BH_4^-$ (−0.48 V) [16,20]. This indicates that Cu^{2+} and In^{3+} ions can be reduced via $NaBH_4$ addition. The formation of Cu–In alloys is attributed possibly to high activities of metallic Cu and In nanoparticles, which facilitate the reactions of Cu and In with each other [21]. The microstructures of the obtained powders are shown in the inset of Fig. 1. The size of particles was in the range of 50–70 nm, indicating that the nanoparticles were formed.

3.2. Characterization and microstructures of the selenized thin films

The pastes containing the prepared nanopowders were coated on soda lime glass (SLG) substrates via the doctor-blading method, followed by the selenization of the desiccated thin films. The XRD

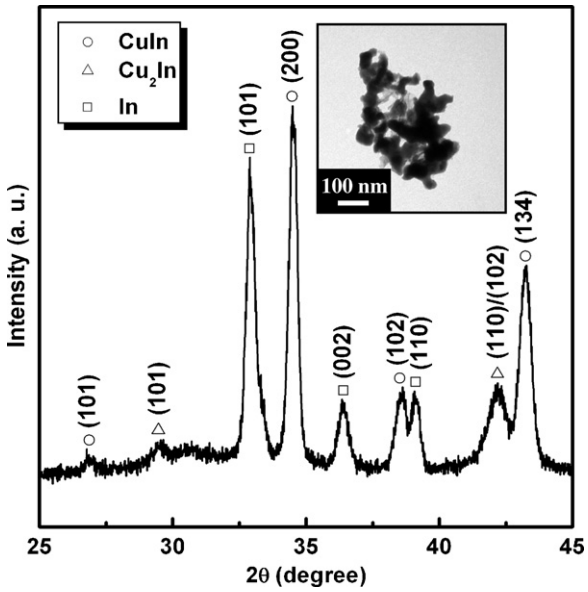

Fig. 1. X-ray diffraction pattern and corresponding transmission electron micrograph of the nanopowders synthesized via the $NaBH_4$-assisted chemical reduction method.

patterns of the selenized films are illustrated in Fig. 2. On the as-coated thin film, CuIn, Cu_2In, and In were found to coexist (Fig. 2(a)). As the selenization temperature was raised to 250 °C (Fig. 2(b)), the peak intensity of Cu_2In phase increased and that of In phase decreased. In addition, the formation of In_2O_3 and Cu was observed. When the temperature was increased to 350 °C (Fig. 2(c)), $CuInSe_2$ was formed. Simultaneously, the peak intensity of In_2O_3 phase diminished. With raising the temperature to 450 °C (Fig. 2(d)), monophasic $CuInSe_2$ was obtained. As the temperature was further increased to 550 °C (Fig. 2(e)), the crystallinity of $CuInSe_2$ phase was improved. The XRD patterns of $CuInSe_2$ were in agreement with the data in ICDD files (No. 89-5648). The formation of $CuInSe_2$

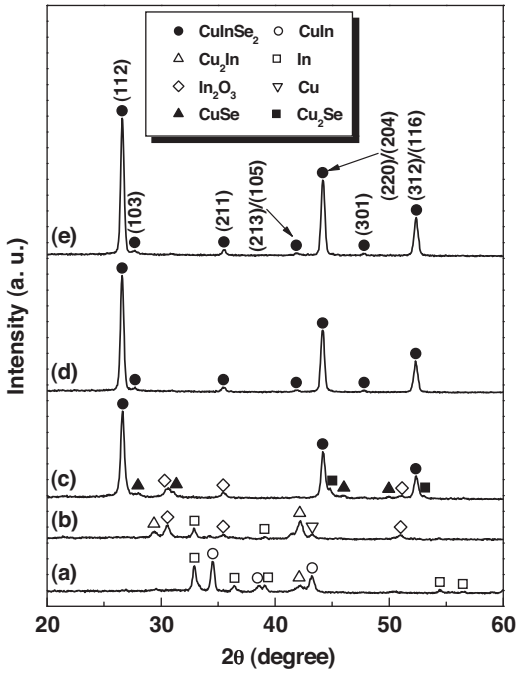

Fig. 2. X-ray diffraction patterns of the thin films selenized at (a) 25 °C (as-coated), (b) 250 °C, (c) 350 °C, (d) 450 °C, and (e) 550 °C for 30 min.

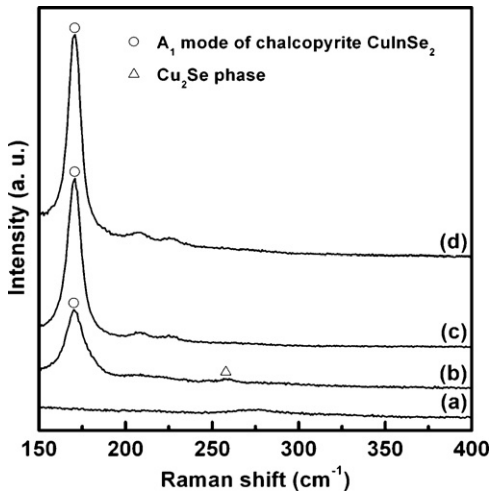

Fig. 3. Raman spectra of the thin films selenized at (a) 250 °C, (b) 350 °C, (c) 450 °C, and (d) 550 °C for 30 min.

with a chalcopyrite structure (α-$CuInSe_2$) was identified from the existence of (1 0 3), (2 1 1), and (2 1 3)/(1 0 5) planes [22].

The Raman spectra of the thin films selenized at various temperatures for 30 min are shown in Fig. 3. Upon selenization at 250 °C (Fig. 3(a)), no Raman peaks were obtained. When the temperature was raised to 350 °C (Fig. 3(b)), a Raman peak at 171 cm^{-1} was observed. According to the report in literature [23], an A_1 mode phonon peak at 171 cm^{-1} in Raman spectra is assigned to chalcopyrite $CuInSe_2$. The A_1 mode phonon results from the interaction of Se atoms in motion with Cu and In atoms at rest [23]. In addition, a Raman peak at 258 cm^{-1} assigned to Cu_2Se phase was also found [24]. Upon selenization at 450 °C (Fig. 3(c)) and 550 °C (Fig. 3(d)), only the Raman peak belonging to chalcopyrite $CuInSe_2$ was detected, indicating that single-phase chalcopyrite $CuInSe_2$ was successfully synthesized. The compositions of the selenized $CuInSe_2$ films after KCN etching were investigated via EDS analysis. The atomic ratios of cupper species to indium species to selenium species were 0.97:1:1.94.

The Rietveld refinement technique was utilized to identify the crystal system, space group, and lattice constants of the $CuInSe_2$ thin films. The refined XRD pattern of the thin film selenized at 550 °C for 30 min is illustrated in Fig. 4. The "×" marks and the solid curve indicate the experimental data and the simulated data,

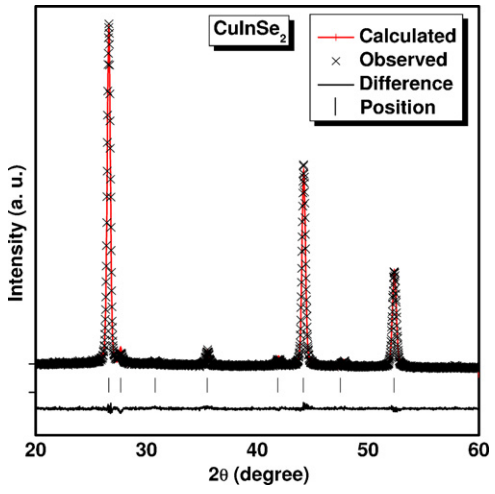

Fig. 4. Refined XRD pattern of the thin film selenized at 550 °C for 30 min via the Rietveld refinement method.

Table 1
Rietveld refinement results of the thin film selenized at 550 °C for 30 min.

Formula	$CuInSe_2$
Crystal system	Tetragonal
Space group	*I*-42*d*
Lattice constants	
a (Å)	5.781
c (Å)	11.612
$\eta = c/2a$	1.004
Cell volume (Å^3)	388.073
R values	
R_{wp} (%)	5.83
R_p (%)	4.03

respectively. (For interpretation of the references to color in the text, the reader is referred to the web version of the article.) The vertical bars show the position of the simulated diffraction peaks, and the black line represents the deviation of the experimental data from the simulated data. The Rietveld refinement results of the $CuInSe_2$ thin film are listed in Table 1. The values of R_{wp} and R_p were 5.83% and 4.03%, respectively, suggesting that the refinement results of the thin film were reliable. The lattice parameter η ($\eta = c/2a$) was calculated to be 1.004, which was consistent with the reported data (ICDD Card No. 89-5648).

To measure the band gap of $CuInSe_2$, the absorbance spectra of the thin film were analyzed. The band gap of the $CuInSe_2$ thin film was calculated from the data of optical absorbance according to the following equation [25]:

$$\alpha h\nu = k(h\nu - E_g)^{1/2} \quad (1)$$

where α is the absorption coefficient, k is a constant, $h\nu$ is the photon energy, and E_g is the energy of band gap. The band gap was estimated via plotting $(\alpha h\nu)^2$ versus $h\nu$. The extrapolation of the straight data line in the plot to $(\alpha h\nu)^2 = 0$ indicates the value of the energy of band gap. The optical band gap of the thin film selenized at 550 °C for 30 min was 0.97 eV as shown in Fig. 5. This value was approximately equal to the value in the reported literature [2].

The microstructures of the thin films selenized at various temperatures for 30 min are illustrated in Fig. 6. After the selenization at 250 °C and 350 °C, the sizes of particles did not change significantly (Fig. 6(a) and (b)). As the temperature was increased to 450 °C (Fig. 6(c)), the particle sizes were enormously enlarged to about 1 μm. It is attributed to the formation of Cu–Se phases existing as fluxing agents [26]. When the selenization temperature was further raised to 550 °C (Fig. 6(d)), the densified chalcopyrite $CuInSe_2$ thin films with a large grain size of 2 μm were successfully prepared. An atomic force micrograph of the heated films has been also shown

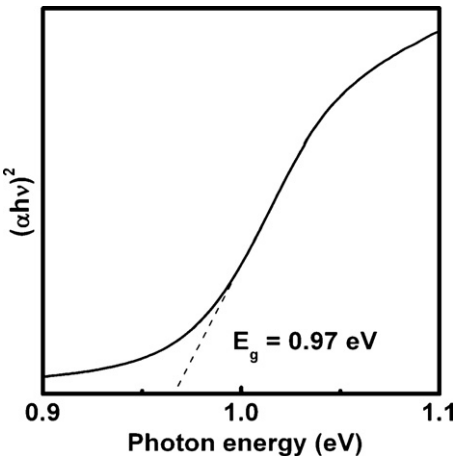

Fig. 5. Absorbance spectra of the thin film selenized at 550 °C for 30 min.

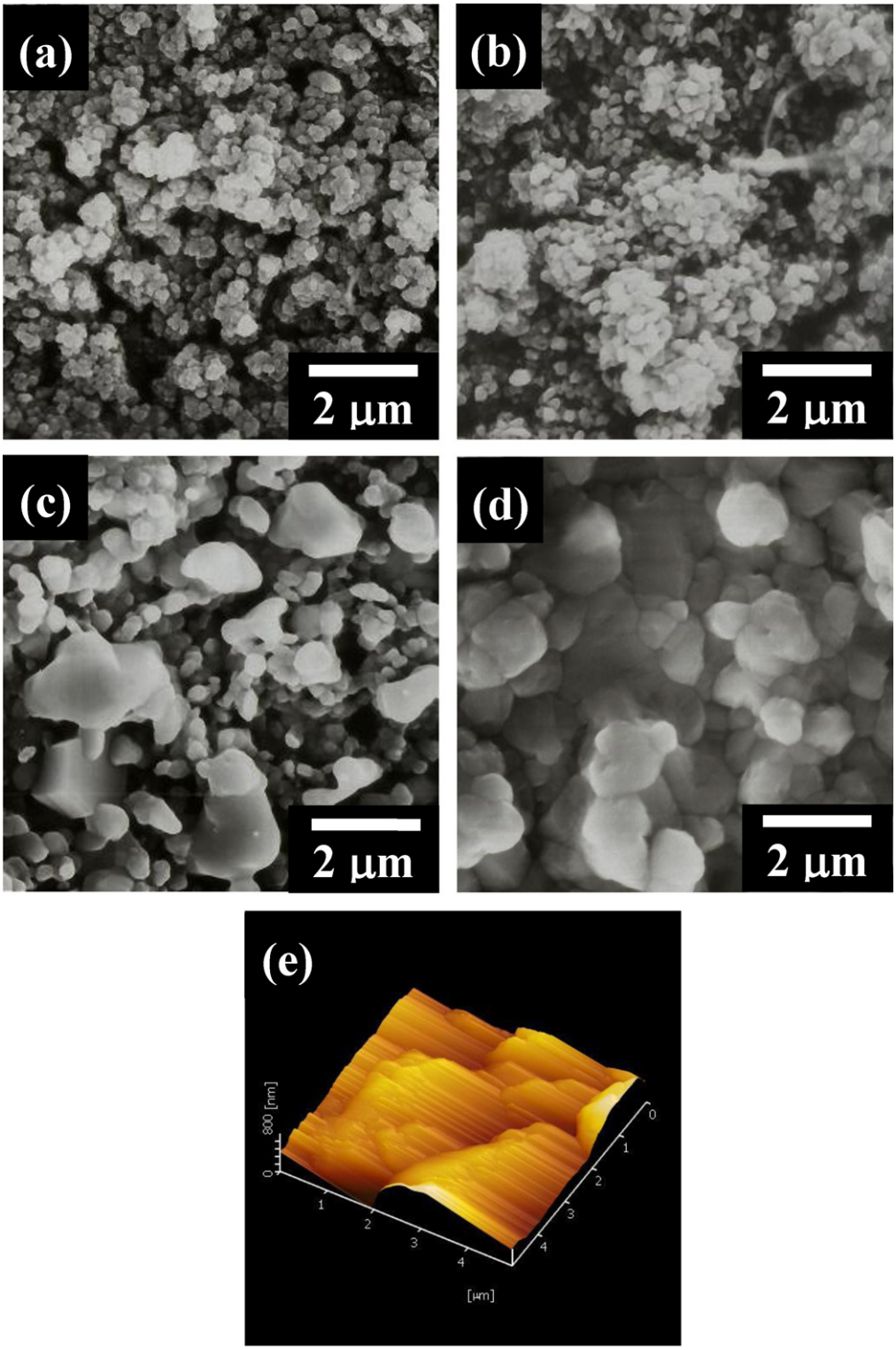

Fig. 6. Scanning electron micrographs of the thin films selenized at (a) 250 °C, (b) 350 °C, (c) 450 °C, (d) 550 °C for 30 min, and (e) atomic force micrographs for the 550 °C–heated films.

in Fig. 6(e). The root-mean-square (RMS) roughness was approximately 96 nm, revealing that $CuInSe_2$ films had a uniform surface morphology and a low RMS roughness.

To examine the variation in composition in various depths of the thin films in which $CuInSe_2$ was formed, grazing incident X-ray diffraction (GIXD) was employed. When the incident angle of the X-ray beam (ω) is much larger than the critical angle (ω_c), below which the total reflection of X-ray occurs, the penetration depth of an X-ray beam into the thin film can be estimated according to the following equation [27]:

$$D(\omega) = \frac{\sin(\omega)}{\mu} \quad (2)$$

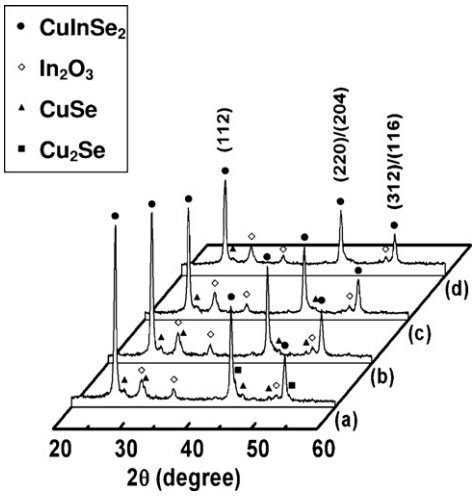

Fig. 7. Grazing incident X-ray diffraction patterns of the thin film selenized at 350 °C for 30 min with the incident angle (ω) of the X-ray beam at (a) 3°, (b) 6°, (c) 9°, and (d) 12°.

where D is the penetration depth of an X-ray beam, and μ is the X-ray linear absorption coefficient of the material. The linear absorption coefficient (μ) of $CuInSe_2$ was calculated to be 757.75 cm^{-1} according to the literature [1,28]. When the incident angles of the X-ray beam (ω) were set at 3°, 6°, 9°, 12°, and 15°, the penetration depths of the X-ray beam into the $CuInSe_2$ thin film ($D(\omega)$) were 0.69, 1.38, 2.06, 2.74, and 3.42 μm, respectively.

The GIXD patterns of the thin films selenized at 350 °C, 450 °C, and 550 °C for 30 min are depicted in Figs. 7–9, respectively. When the selenization temperature was 350 °C (Fig. 7), $CuInSe_2$ and In_2O_3 were formed throughout the thin film. Simultaneously, Cu_2Se and CuSe were observed near the surface of the thin film. It is considered that the reaction of Cu–In alloy with Se results in the formation of $CuInSe_2$. The formation of $CuInSe_2$ throughout the thin films at 350 °C implies that the reactivities of the synthesized nanoparticles with Se vapor are high. Simultaneously, Cu species react with Se vapor to form Cu–Se phases near the surface of the thin film. The presence of In_2O_3 is attributed to the reaction of indium with oxygen existing in the solvent of the prepared pastes. With further increasing the temperature to 450 °C (Fig. 8), In_2O_3 was found to coexist in the thin film except in the vicinity of the surface. After the thin film was selenized at 550 °C (Fig. 9), monophasic

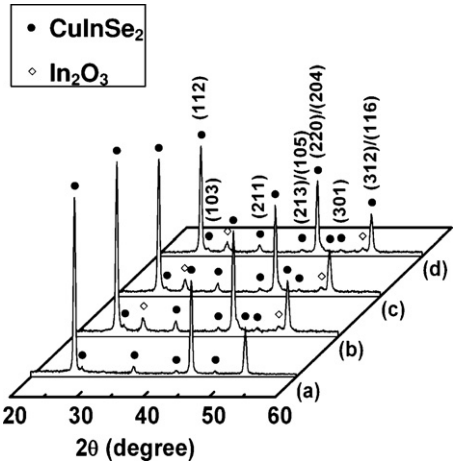

Fig. 8. Grazing incident X-ray diffraction patterns of the thin film selenized at 450 °C for 30 min with the incident angle (ω) of the X-ray beam at (a) 3°, (b) 6°, (c) 9°, and (d) 12°.

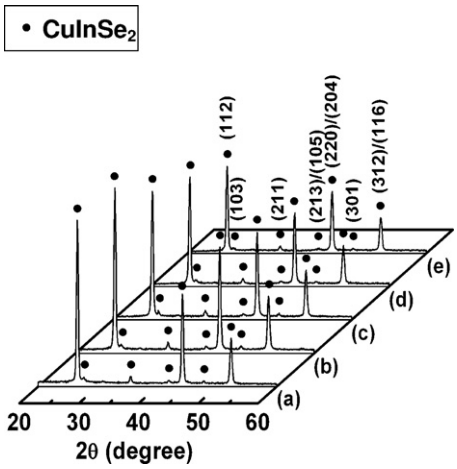

Fig. 9. Grazing incident X-ray diffraction patterns of the thin film selenized at 550 °C for 30 min with the incident angle (ω) of the X-ray beam at (a) 3°, (b) 6°, (c) 9°, (d) 12°, and (e) 15°.

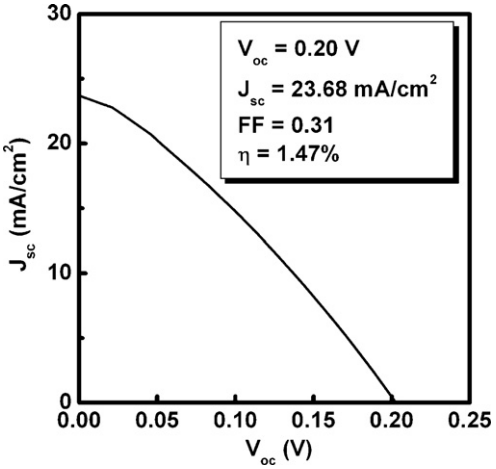

Fig. 10. Current–voltage characteristics of the fabricated $CuInSe_2$ thin film solar cell under AM 1.5 G illumination.

chalcopyrite $CuInSe_2$ phase was obtained throughout the thin film without impurity phases remaining near the substrate. It is inferred that at elevated temperatures the diffusion of Se vapor within the thin film is enhanced correspondingly [29,30], thereby facilitating the formation of the single-phase $CuInSe_2$ thin film. A monophasic $CuInSe_2$ thin film was successfully prepared via selenizing the obtained nanopowders.

3.3. Characterization of the $CuInSe_2$ thin-film solar cell

The thin films selenized at 550 °C for 30 min were utilized to fabricate solar cells. Current–voltage characteristics of the ITO/i-ZnO/CdS/$CuInSe_2$/Mo/SLG thin-film solar cell under AM 1.5 G (100 mW/cm^2) illumination are shown in Fig. 10. The efficiency (η) of the solar cell was 1.47% (active area = 0.07 cm^2) with open-circuit voltage (V_{oc}), short-circuit current density (J_{sc}), and fill factor (FF) values of 0.20 V, 23.68 mA/cm^2, and 0.31, respectively. Well-performed J_{sc} value is attributed to compact grains in the $CuInSe_2$ thin films. $CuInSe_2$ thin-film solar cells were demonstrated to be fabricated via coating the prepared nanopowders combined with the selenization process.

4. Conclusions

$CuInSe_2$ thin films were prepared using nanopowders as the precursors of selenization. Nanopowders consisting of Cu–In alloys and In with a size of about 50–70 nm were synthesized in water via the $NaBH_4$-assisted chemical reduction method. These nanopowders were obtained at relatively low temperatures in ambient atmosphere using readily available, low-toxic compounds as starting materials. During the selenization at 350 °C, $CuInSe_2$ started to form and coexisted with copper selenides. The particle sizes of the thin films were significantly enlarged at 450 °C owing to the presence of Cu–Se phases. The densified $CuInSe_2$ films with a grain size of around 2 μm were prepared on selenization at 550 °C. Grazing incident X-ray diffraction demonstrated that monophasic $CuInSe_2$ was formed throughout the thin film. The formation of $CuInSe_2$ with a pure chalcopyrite structure was confirmed via Raman spectroscopy and the Rietveld refinement analysis. The band gap energy of the $CuInSe_2$ was 0.97 eV measured via UV–visible–NIR spectroscopy. The overall photovoltaic conversion efficiency of the $CuInSe_2$ thin-film solar cells was 1.47% under AM 1.5 G illumination.

Acknowledgements

The authors would like to thank the National Science Council, Taiwan, the Republic of China, for partial financial support of this study under Contract No. NSC 100-3113-E002-011.

References

[1] E.J. Lee, J.W. Cho, J.H. Kim, J.H. Yun, J.H. Kim, B.K. Min, J. Alloys Compd. 506 (2010) 969–972.
[2] S. Schleussner, U. Zimmermann, T. Wätjen, K. Leifer, M. Edoff, Sol. Energy Mater. Sol. Cells 95 (2011) 721–726.
[3] M.A. Green, K. Emery, Y. Hishikawa, W. Warta, Prog. Photovolt: Res. Appl. 18 (2010) 144–150.
[4] S. Seyrling, A. Chirila, D. Güttler, P. Blösch, F. Pianezzi, R. Verma, S. Bücheler, S. Nishiwaki, Y.E. Romanyuk, P. Rossbach, A.N. Tiwari, Sol. Energy Mater. Sol. Cells 95 (2011) 1477–1481.
[5] J.A. Frantz, R.Y. Bekele, V.Q. Nguyen, J.S. Sanghera, A. Bruce, S.V. Frolov, M. Cyrus, I.D. Aggarwal, Thin Solid Films 519 (2011) 7763–7765.
[6] G. Norsworthy, C.R. Leidholm, A. Halani, V.K. Kapur, R. Roe, B.M. Basol, R. Matson, Sol. Energy Mater. Sol. Cells 60 (2000) 127–134.
[7] B.M. Basol, Thin Solid Films 361–362 (2000) 514–519.
[8] V.K. Kapur, A. Bansal, P. Le, O.I. Asensio, Thin Solid Films 431–432 (2003) 53–57.
[9] M. Kaelin, D. Rudmann, F. Kurdesau, H. Zogg, T. Meyer, A.N. Tiwari, Thin Solid Films 480–481 (2005) 486–490.
[10] S.M. Wu, Y.Z. Xue, Z.H. Zhang, J. Alloys Compd. 491 (2010) 456–459.
[11] F.Y. Liu, C. Huang, Y.Q. Lai, Z. Zhang, J. Li, Y.X. Liu, J. Alloys Compd. 590 (2011) L129–L133.
[12] W.W. Hou, B. Bob, S.H. Li, Y. Yang, Thin Solid Films 517 (2009) 6853–6856.
[13] M. Yuan, D.B. Mitzi, O. Gunawan, A.J. Kellock, S.J. Chey, V.R. Deline, Thin Solid Films 519 (2010) 852–856.
[14] L.Y. Hsiao, J.G. Duh, J. Electrochem. Soc. 152 (2005) J105–J109.
[15] M.V. Orta, D. Diaz, P.S. Jacinto, A.V. Olmos, E. Reguera, J. Phys. Chem. B 112 (2008) 14427–14434.
[16] N.H. Chou, X. Ke, P. Schiffer, R.E. Schaak, J. Am. Chem. Soc. 130 (2008) 8140–8141.
[17] J.Y. Chang, J.H. Lee, J.H. Cha, D.Y. Jung, G.B. Choi, G.Y. Kim, Thin Solid Films 519 (2011) 2176.
[18] G.B. Chen, L. Wang, X. Sheng, D. Yang, J. Mater. Sci.: Mater. Electron. 22 (2011) 1124.
[19] D.V. Goia, J. Mater. Chem. 14 (2004) 451–458.
[20] T. Ishizaki, N. Saito, A. Fuwa, Mater. Trans. 40 (1999) 867–870.
[21] P.V. Kamat, J. Phys. Chem. B 106 (2002) 7729–7744.
[22] A. Gupta, S. Shirakata, S. Isomura, Sol. Energy Mater. Sol. Cells 32 (1994) 137–149.
[23] V. Izquierdo-Roca, R. Caballero, X. Fontané, C.A. Kaufmann, J. Álvarez-García, L. Calvo-Barrio, E. Saucedo, A. Pérez-Rodríguez, Thin Solid Films 519 (2011) 7300–7303.
[24] B.M. Sukarova, M. Najdoski, I. Grozdanov, C.J. Chunnilall, J. Mol. Struct. 410–411 (1997) 267–270.
[25] L. Oliveira, T. Todorov, E. Chassaing, D. Lincot, J. Carda, P. Escribano, Thin Solid Films 517 (2009) 2272–2276.
[26] C.H. Wu, F.S. Chen, S.H. Lin, C.H. Lu, J. Alloys Compd. 509 (2011) 5783–5788.
[27] C.H. Lu, C.Y. Wen, J. Appl. Phys. 86 (1999) 6335–6341.
[28] B.D. Cullity, S.R. Stock, Elements of X-ray Diffraction, third ed., Prentice Hall, Upper Saddle River, NJ, USA, 2001, pp. 11–12, 630–631.
[29] F. Jiang, J. Feng, Thin Solid Films 515 (2006) 1950–1955.
[30] A. Parretta, M.L. Addonizio, S. Loreti, L. Quercia, M.K. Jayaraj, J. Cryst. Growth 183 (1998) 196–204.